PERGAMON

Vision Research 39 (1999) 2031–2037

Vision Research

Rapid communication

Measurement of the eye's near infrared wave-front aberration using the objective crossed-cylinder aberroscope technique

Norberto López-Gil [a,b,*], Howard C. Howland [a]

[a] *Section of Neurobiology and Behavior, Cornell University, Ithaca, NY 14853, USA*
[b] *Laboratorio de Óptica, Departamento de Física, Universidad de Murcia, Campus de Espinardo (Edificio C), 30071 Murcia, Spain*

Received 24 September 1998; received in revised form 26 November 1998

Abstract

We used the crossed-cylinder aberroscope technique to obtain the near infrared (784 nm) wave-front aberration of the human eye. We compared the results with those obtained under the same conditions using red light (633 nm). Other than the greater retinal scattering of the near infrared light, third- and fourth-order wave-front aberrations are similar in both wavelengths. Values of the calculated near infrared point spread function show a typical half-height width of around 2 arcmin, which is in good agreement with previous work. © 1999 Elsevier Science Ltd. All rights reserved.

Keywords: Aberration; Human eye; Near infrared

1. Introduction

In recent years, several researchers have used different techniques to make in vivo measurements of the monochromatic wave-front aberration of the human eye (Webb, Penney & Thompson, 1992; Howland & Howland, 1976; Liang, Grimm, Goelz & Billie, 1994). In all cases, the measurements have been done in visible light using a wavelength of 543 or 632.8 nm from He–Ne lasers. A recent work has shown the possibility of using near infrared light (NIRL) in double pass measurements of the optical performance of the eye (López-Gil & Artal, 1997). Values of the eye's modulation transfer function (MTF) with visible and NIRL are very similar once the different diffraction effects produced for each wavelength have been overcome. As a consequence, NIRL has been used to estimate the optical performance of the eye as a function of accommodation (López-Gil, Iglesias & Artal, 1998).

The objective measurement of the wave-front error using NIRL has the advantage of being more comfortable for the subject because no cycloplegia is required. Moreover, a smaller irradiance is needed when using NIRL because of the higher retinal reflectance (Delori & Pflibsen, 1989). However, the use of NIRL to obtain reliable data on the eye's wave-front aberration may be limited by such factors as the eye's chromatic aberration and different diffraction effects, which could cause the wave-front to differ from one obtained in visible light.

The two main goals of this work are: (1) to show that it is possible to measure the wave-front aberration with NIRL using an objective technique; and (2) to compare the NIRL wave-front with the visible light wave-front in the same subjects under the same experimental conditions.

2. Methods

We used the objective crossed-cylinder aberroscope technique (Walsh, Charman & Howland, 1984) to measure the eye's wave-front aberration. A square grid placed between two crossed-cylinders is projected at the entrance pupil of the eye. Fig. 1 represents the experimental set-up.

* Corresponding author. Tel.: +34-968-367222; fax: +34-968-363528; e-mail: norberto@fcu.um.es.

PII: S0042-6989(98)00315-0

In Fig. 1, the intensity of the red light coming from the He–Ne laser, V-L, is reduced by a neutral density filter, NF, and spatially filtered by a microscope objective and a pinhole aperture, SF, which is placed at the focal plane of the collimator C. After two reflections the light arrives at the crossed cylinder aberroscope, A. The magnification system, MS, and the beam splitter, BS2, help to conjugate the aberroscope with the subject's pupil which can be corrected by using a trial lens TL. LT acts as a light trapper to avoid reflections and the CCD camera captures the light coming out the eye after it has been reflected by the retina. PS are positioners to center the subject's pupil with respect the stop, S, and the aberroscope. The near infrared light coming from the laser diode, IR-L, was already collimated, however, due to the small diameter of the beam it has been used an beam expander, BE. Another beam splitter, BS1, is used to force the near infrared light to have the same path as the red one.

The irradiance at the plane of the cornea was well within safe standards (ANSI Z136.1, 1993) for the typical exposure time (3 s) and the wavelengths used (633 and 784 nm). The grid is distorted at the subject's retinal plane due to the aberrations of the eye. The aberration also blurs the lines forming the grid. Part of the light reflected by the retina exits after a double pass through the eye and is captured by a CCD camera (see Fig. 1). Aberrations of the eye cause each single point of the retinal image of the grid to spread again in the second pass but the grid is not re-distorted in this pass. Therefore an analysis of the grid distortion in the final images reveals the eye's wave-front aberration.

The experimental set-up represented in Fig. 1 has been calibrated and used to obtain the wave-front aberration of a system that generated third-order spherical and coma aberration (López-Gil, Howland, Howland, Charman & Applegate, 1998). To obtain the correct coefficients of the wave-front aberration, it is important to calibrate the system with precise knowledge of the grid spacing at the entrance plane of the pupil. This spacing is measured empirically by placing the CCD camera (without objective) at the same plane as the entrance plane of the subject's pupil. In our case the spacing was 862 μm.

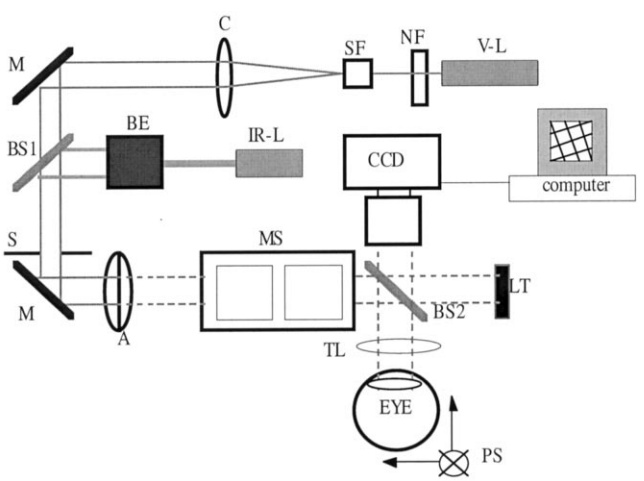

Fig. 1. Experimental set-up. V-L, He–Ne laser (632.8 nm); NF, neutral density filter; SF, spatial filter; C, collimator; M, mirror; BS, beam splitter; IR-L, near infrared laser diode (784 nm); BE, beam expander; S, iris stop; A, aberroscope; MS magnification system (M = 1); TL, trial lens; PS positioners; LT, light trapper; CCD camera. The aberroscope plane and the subject's pupil plane are conjugated by means of MS.

Prior to analyzing the aberroscopic images, it is necessary to perform digital processing to find the intersections of the grid. Although this procedure is not necessary for the red images, it must be used with the near infrared ones because of the higher retinal scattering.

Grid distortions produced by the same wave-front aberration can show totally different values of coma when different grid centers are used. Therefore, in order to compare the red and near infrared results, it is necessary to find a common axis to which the wave-front aberration can be referred. The grid center cannot be used because the alignment between the optical system and the eye could change slightly in each measurement. However, a small misalignment will not affect the grid distortion with respect to the pupil. For that reason, a possible solution is to use a reference point that takes into account the subject's pupil geometry. Considering that pupil size limits the retinal surface illuminated by the light from the aberroscope, we have used an algorithm on the binarized aberroscopic image and found its centroid. This point has been used as the reference point. Once this center is located, the grid distortion is analyzed and the wave-front aberration at the entrance pupil is calculated in terms of Taylor coefficients up to the fourth-order.

Measurements were taken on three subjects aged 19 (GJ and GW) and 31 (KE). One subject was emmetropic (GW) and the others were corrected with trial lenses of -3.5 D (GJ) or -3 D/-1.25 D@90 (KE). As demonstrated before (López-Gil et al., 1998), the overall radial profile of the eye's MTF remains similar with accommodation, but the wave-front aberration can change depending on accommodative state (Atchison, Collins, Wildsoet, Christensen & Waterworth, 1995). To assure that the refractive state remained the same with both wavelengths, the subject's accommodation was paralyzed with two drops of a mild cycloplegic (tropycamide 0.5%).

3. Results

Fig. 2 represents the aberroscopic patterns for the three subjects and both wavelengths.

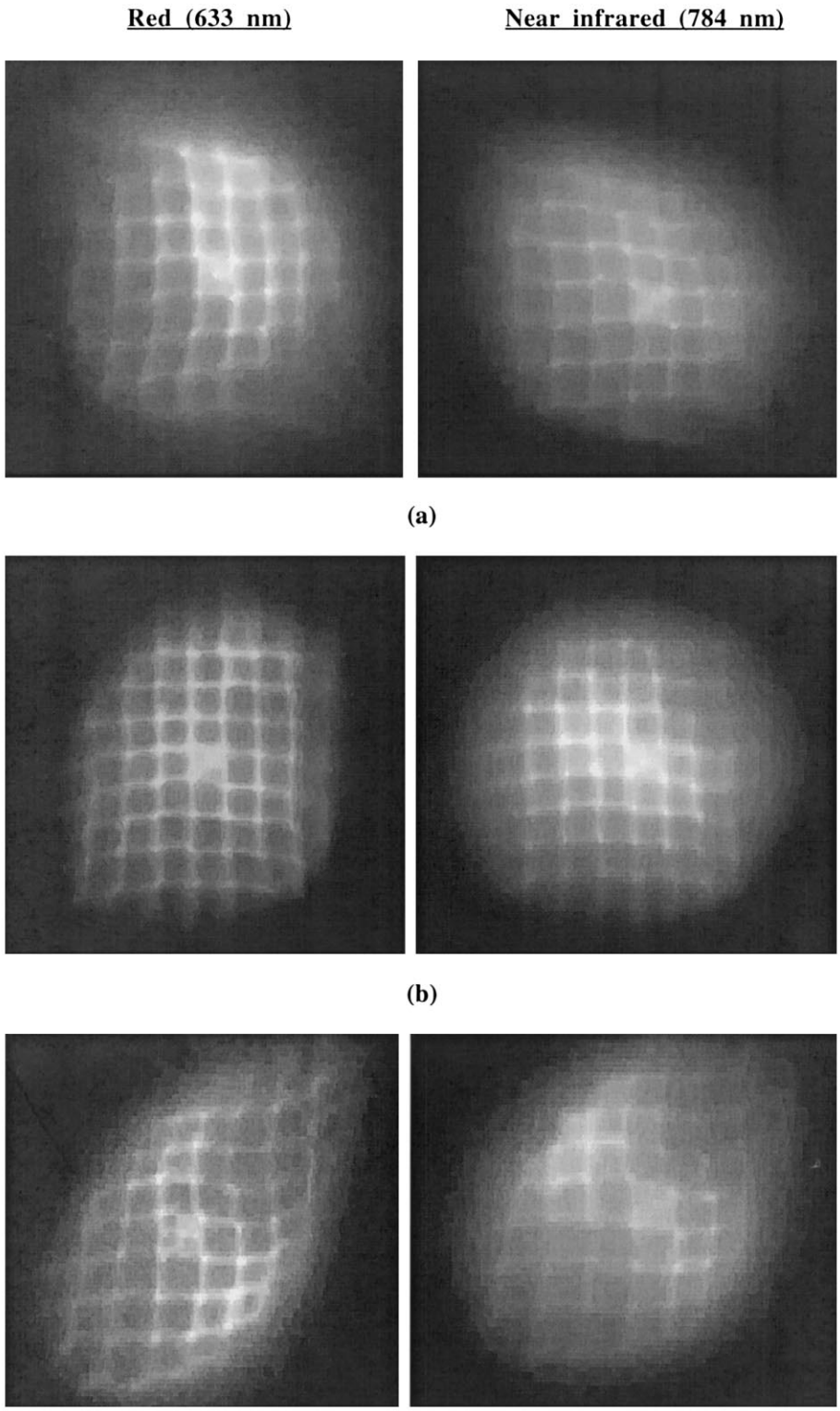

Fig. 2. Aberroscopic retinal images of subject GJ (a), GW (b) and KE (c), obtained using a crossed cylinder aberroscope with red light (left column) and near infrared light (right column). The angle represented is nearly 2.5 deg of arc. The images have been digitally processed to avoid noise and to sharpen the lines.

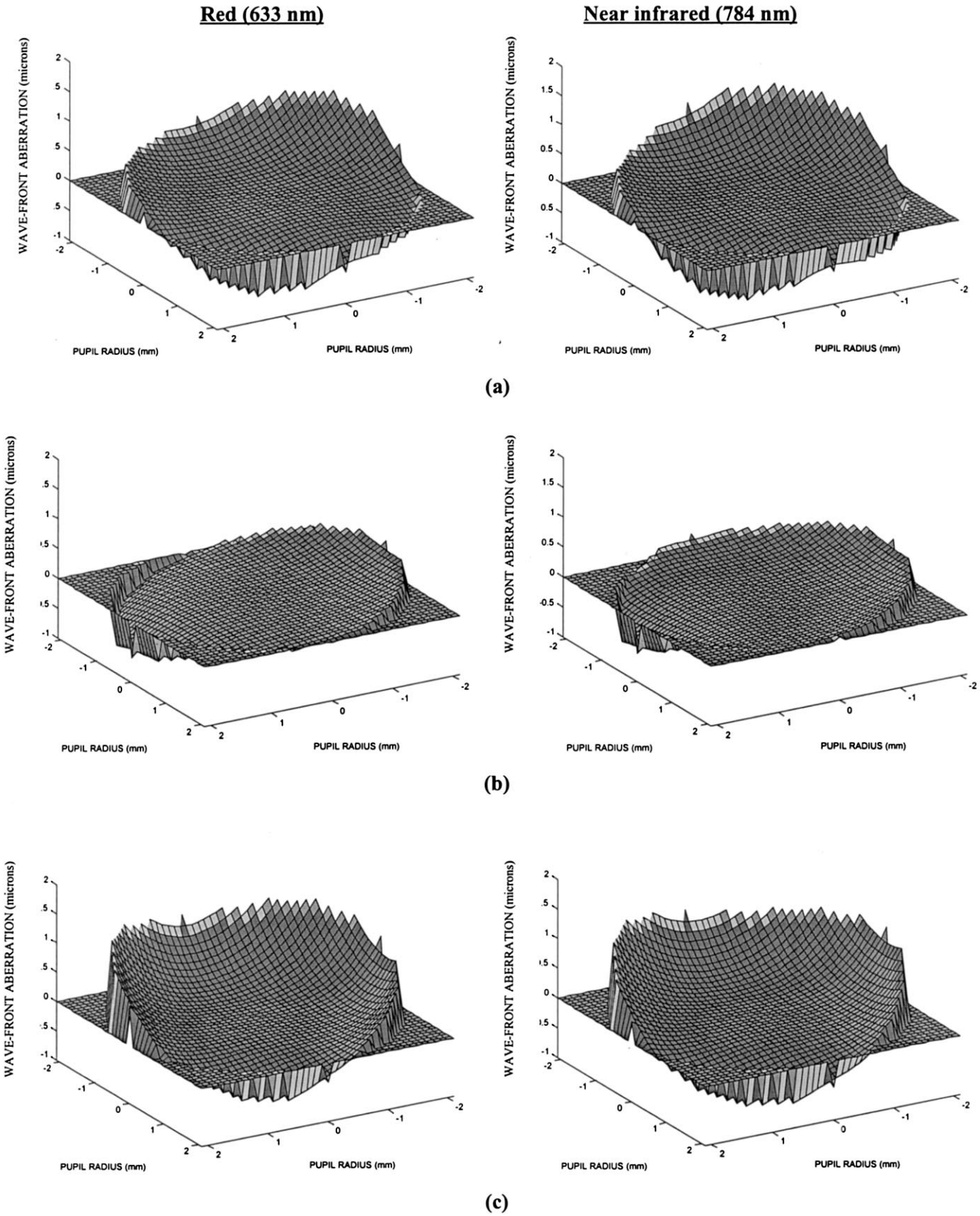

Fig. 3. Wave-front aberration of subject GJ (a), GW (b) and KE (c) using measurements obtained with red light (first column) and near infrared light (second column). Represented here are only the third- and fourth-order terms of the Taylor expansion of the wave-front for a 4.2 mm diameter pupil. For clarity, all the surfaces have been rotated 180° with respect to the Z-axis.

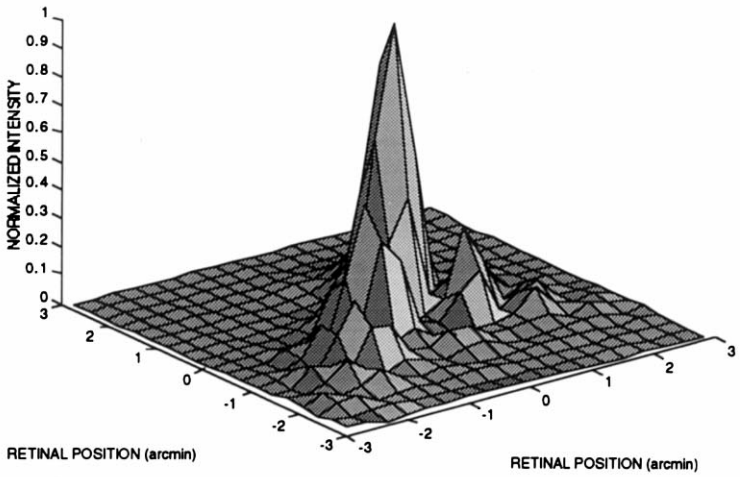

(a)

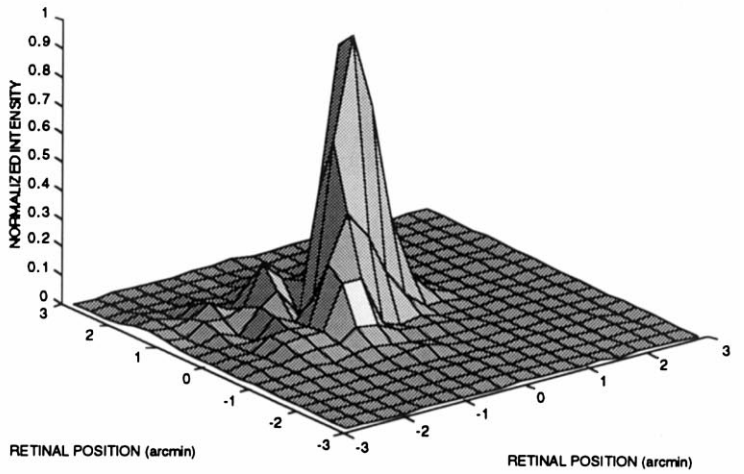

(b)

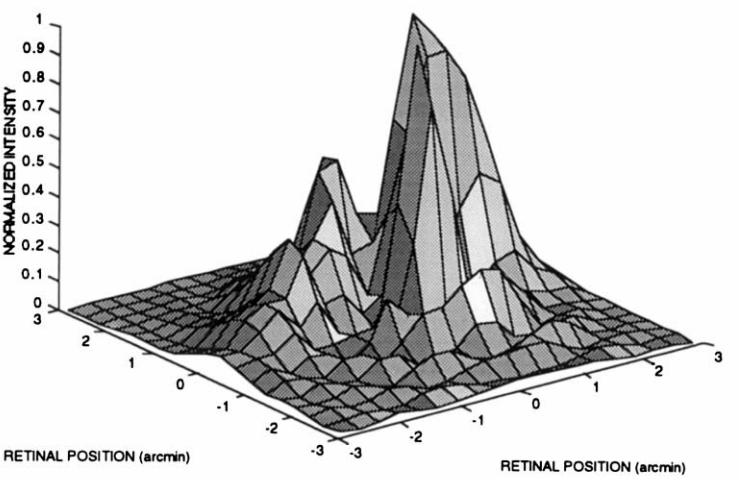

(c)

Fig. 4. Central part of the normalized near infrared PSF for subjects GJ (a), GW (b) and KE (c) for a 4.2 mm diameter pupil.

On first inspection, the distortions of the grid are similar for each subject when using both wavelengths, and the near infrared aberroscopic patterns are less well defined than the red ones, mainly due to the retinal scattering which produce an halo on the retinal image.

Intersections of 6×6 (GJ), 5×5 (GW and KE) out the original grid size, 8×8, have been analyzed within the limitations imposed by pupil size, aberrations, and the Stiles-Crawford effect. Fig. 3 represents the red and near infrared wave-front aberration for each subject.

Fig. 4 shows the central part of the near infrared point spread function (PSF) calculated as the square modulus of the Fourier transform of the pupil function (Goodman, 1996).

4. Discussion and conclusion

Aberroscopic images of the human eye have been recorded using near infrared light (784 nm). After digital processing, the images are good enough to be analyzed and used to calculate the eye's near infrared wave-front aberration. Comparing these images with the aberroscopic images obtained with red light (633 nm) shows that the grid is distorted in a similar pattern. However, about a 20% reduction in contrast of the near infrared images was found because of the higher retinal scattering and possible reflections in other retinal layers (Elsner, Burns, Hughes & Webb, 1992). Using the near infrared wave-front aberration values we computed the width of the grid lines after double pass. A comparison with the real width of the grid lines on the near infrared aberroscopic images shows that the additional width is due to such extra-optical effects as retinal scattering.

The average value of the width at half-height of the core part of the near infrared PSF (single pass) is a little less than 2 min of arc (see Fig. 4). Using the near infrared wave-front aberration calculated as the correlation between the PSF of each pass (Artal, Iglesias, López-Gil & Green, 1995) we have found that the width of the simulated double pass images of a point source is in close agreement with the one obtained experimentally using the double-pass technique (López-Gil & Artal, 1997). In both cases, the width is about 3 min of arc. The resolution of an optical system is limited by the size of its PSF, so the maximum size of the area at half-height represents a parameter that must be taken into account when designing an optical instrument that calls for near infrared light to be applied in the eye. The advantage of computing the double-pass image directly from the wave-front aberration is that the increase of the backscattering area only reduces image quality leaving the result unaltered, while in the double-pass method this effect could be interpreted as an increase of the size of the PSF due to poor optical performances.

Further comparison of the aberroscopic images shows inter-subject variation of the wave-front aberration similar to that found in previous works (Howland & Howland, 1976; Lu, Munger & Campbell, 1993; Atchison et al., 1995). In this particular study, coma and third-order spherical aberration are dominant for subjects GJ and KE, respectively, while subject GW has few aberrations.

Red and near infrared aberroscopic patterns reveal similar higher-order aberration coefficients with the two wavelengths. A better agreement was found in spherical aberration due to its insensitivity to small errors in locating the pupil center.

To our knowledge, this is the first time the wave-front aberration of the human eye has been measured using near infrared light with the crossed cylinder aberroscope technique. Using this wavelength, 784 nm, together with a fast method of calculating the wave-front aberration will allow us to study the real-time changes in wave-front as in the eye's optical changes during accommodation (Jofer, Porter & Williams, 1998).

Acknowledgements

We wish to thank Melissa Hergan for her help with the measurements and Pablo Artal for his suggestions on the manuscript. This work was supported by NIH EY02994 to HCH and by a postdoctoral fellowship from the Spanish Ministerio de Educación y Cultura to N. López-Gil.

References

Artal, P., Iglesias, I., López-Gil, N., & Green, D. G. (1995). Double-pass measurements of the retinal-image quality with unequal entrance and exit pupil sizes and the reversibility of the eye's optical system. *Journal of the Optical Society of America A*, *12*, 2358–2366.

Atchison, D. A., Collins, M. J., Wildsoet, C. F., Christensen, J., & Waterworth, M. D. (1995). Measurement of monochromatic ocular aberrations of human eyes as a function of accommodation by the Howland aberroscope technique. *Vision Research*, *35*, 313–323.

Delori, F. C., & Pflibsen, K. P. (1989). Spectral reflectance of the human ocular fundus. *Applied Optics*, *28*, 1061–1077.

Elsner, A. E., Burns, S. A., Hughes, G. W., & Webb, R. H. (1992). Reflectometry with a scanning laser ophthalmoscope. *Applied Optics*, *31*, 3697–3710.

Goodman, J. W. (1996). *Introduction to Fourier optics* (2nd). New York: McGraw-Hill.

Howland, B., & Howland, H. C. (1976). Subjective measurement of high-order aberrations of the eye. *Science*, *193*, 580–582.

Jofer, H. J., Porter, J., & Williams, D. R. (1998). *Investigative Ophthalmology and Visual Science* (*Supplement*), *39*, 396.

Liang, J., Grimm, B., Goelz, S., & Billie, J. F. (1994). Objective measurement of wave aberrations of the human eye with the use of a Hartmann-Shack wave-front sensor. *Journal of the Optical Society of America A*, *11*, 1949–1957.

López-Gil, N., & Artal, P. (1997). Comparison of double-pass estimates of the retinal-image quality obtained with green and near-infrared light. *Journal of the Optical Society of America A*, *14*, 961–971.

López-Gil, N., Howland, H. C., Howland, B., Charman, N., & Applegate, R. (1998). Generation of third-order spherical and coma aberrations using radially symmetric fourth-order lenses. *Journal of the Optical Society of America A*, *15*, 2563–2571.

López-Gil, N., Iglesias, I., & Artal, P. (1998). Retinal image quality in the human eye as a function of the accommodation. *Vision Research*, *38*, 2897–2907.

Lu, C., Munger, R., & Campbell, M. C. W. (1993). Monochromatic aberrations in accommodated eyes. *Technical digest series*, *ophthalmic and visual optics*, vol. 3 (pp. 160–163). USA: Optical Society of America.

Walsh, G., Charman, W. N., & Howland, H. C. (1984). Objective technique for the determination of monochromatic aberrations of the human eye. *Journal of the Optical Society of America A*, *1*, 987–992.

Webb, R. H., Penney, C. M., & Thompson, K. P. (1992). Measurement of ocular local wave-front distortion with a spatially resolved refractometer. *Applied Optics*, *311*, 3678–3686.

ANSI Z136.1 (1993). American national standard for the safe use of lasers.